

Dynamics of exciton localization in a CdSe_{0.5}S_{0.5} mixed crystal

H. X. Jiang, L. Q. Zu, and J. Y. Lin

Department of Physics, Cardwell Hall, Kansas State University, Manhattan, Kansas 66506-2601

(Received 9 May 1990; Revised manuscript received 19 July 1990)

Dynamic processes of exciton localization in a CdSe_{0.5}S_{0.5} II-VI mixed semiconductor have been studied by time-resolved photoluminescence. We found experimentally that the exciton transfer rate depicts a power-law behavior near the mobility edge E_m . Our results indicate that the exciton localization radius behaves according to the law $a(E) \sim |E_m - E|^{-s}$ ($E \leq E_m$) with s being nearly equal to 0.7, which is analogous to the behavior of the localized carriers in the Mott-Anderson model. The spectral shift with delay time has been shown to be a natural consequence of the observed exciton-lifetime behavior.

The effects of the random potential fluctuations, which arise from local compositional fluctuations, on exciton luminescence in mixed semiconductor alloys have been investigated by a number of authors.¹⁻⁸ Alloy disorder causes linewidth broadening in exciton emission spectra, which is a consequence of the exciton localization in random potential wells induced by compositional fluctuations. Studies on the exciton-one-LO-phonon band luminescence show that the exciton luminescence line narrows when the excitation energies are tuned below a critical energy E_{cm} , which has been taken as evidence for an effective mobility edge in the Mott-Anderson picture of localization. The origin for the observed phenomenon was thought to be that an exciton created at a point where its energy is greater than E_{cm} will quickly transfer to lower-energy sites by phonon emission and an exciton created below E_{cm} will decay resonantly on the same site.⁴ Time-resolved emission spectra of the one-LO-phonon band also showed that the spectral peak position shifts toward lower emission energies as the delay time increases when the excitation energies are tuned into the zero-phonon-exciton emission band. The spectral shift with delay time becomes more pronounced for higher excitation energies,⁶ which indicates that exciton transfer takes place throughout the entire disorder localization band. Most of the previous work has assumed that the decrease in transfer rate from an increase of localization energy is due to the available density of states decreasing. A boundary condition at which the transfer rate equals the radiative decay rate at a characteristic energy, which lacks physical justification, has also been used in calculations in two previous investigations.^{7,8} In fact, the experimentally measured nonradiative decay rate in extended states is much larger than the radiative decay rate in localized states at low temperatures.⁶

In mixed crystals, a critical energy E_m , which separates the localized and delocalized exciton states in a random potential induced by compositional fluctuations, is expected. Recent investigations on Zn_xCd_{1-x}Se and CdSe_xS_{1-x} mixed crystals have demonstrated that the random local potential fluctuations induced by compositional fluctuations are responsible for persistent photoconductivity (PPC) observed in these materials,⁹⁻¹¹ and a phase transition has been observed, in which the stored charge car-

riers experienced a transition from localized to percolation (delocalized) states. Thus we have directly demonstrated the existence of the mobility edge in mixed crystals. Localization of carriers in the Mott-Anderson model has been described in great detail by Shklovskii and Efros.¹² In this model description, as one approaches the localization threshold from the side of localized states, the localization radius of a charge carrier (electron or hole) should increase sharply, and diverges at the transition point. However, the dependence of the exciton localization radius on the localization energy has never been investigated, which is in fact very important for the understanding of the dynamic processes of exciton localization in disordered systems. In this paper, we found in a CdSe_{0.5}S_{0.5} mixed crystal that the dependence of the exciton transfer rate on the localization energy depicts a power-law behavior near the mobility edge, which is caused predominantly by changes in the exciton localization radius. Such behavior is analogous to that of localized carriers in the Mott-Anderson localization model.¹² The emission spectral-peak position shift with delay time can also be fully understood in terms of our interpretation and is to be shown as a natural consequence of the localization energy dependence of the exciton lifetime.

The sample used for this study was a CdSe_{0.5}S_{0.5} mixed crystal of size 5×10×1 mm³ obtained from Cleveland Crystal Inc. Resistivity of the sample at room temperatures in the dark is about 5×10⁹ Ω cm. The c axis of the sample is perpendicular to the large-area surface. Data were collected in a reflecting mode. Excitation pulses of about 7 ps in duration at a repetition rate of 1 MHz were provided by a cavity-dumped ultrafast dye laser (Coherent 702-2CD) which was pumped by an yttrium-aluminum-garnet (YAG) laser (Quantronix 416) with a frequency doubler. The lasing photon energy was 2.125 eV with a spectral width of about 2 meV corresponding to a band-to-band excitation. The average power density is about 100 mW/cm². The effective time resolution of the system is about 0.2 ns. The sample was mounted strain free inside a closed-cycle He refrigerator and maintained at a temperature of 8.5 K.

Time-resolved photoluminescence emission spectra obtained for three different delay times are plotted in Fig. 1. The luminescence spectra at different delay times, t_d , have

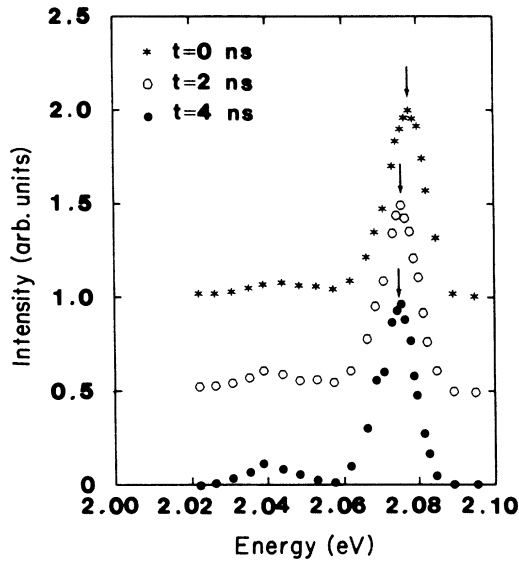


FIG. 1. The low-temperature (8.5 K) time-resolved emission spectra for three different delay times of a CdSe_{0.5}S_{0.5} mixed crystal. The arrows indicate the peak positions at different delay times. The excitation energy was 2.125 eV with an average power density of about 100 mW/cm². The luminescence spectra at different delay times have been rescaled for presentation.

been rescaled for presentation, and $t_d = 0$ has been chosen at the peak positions in the luminescence temporal responses. The arrows indicate the peak positions at different delay times. Two peaks at 2.078 and 2.045 eV in the spectrum of $t_d = 0$ are ascribed, respectively, to the radiative recombination of localized excitons and its one-LO-phonon replica, which are consistent with the emission spectrum obtained for CdS_{0.51}Se_{0.49} (Ref. 13) by considering a linear shift in band gap due to the difference in Se composition. The full width at half maximum (FWHM) is about 11.3 meV, which is predominantly caused by compositional fluctuations. Figure 1 clearly shows that the spectral-peak position shifts toward lower energies as delay time increases. After a pulsed excitation, initially generated free carriers relax to the conduction-band and the valence-band edges to form excitons within about 50 ps.⁵ Our results indicate that the distribution of the exciton population is at thermal equilibrium only at $t_d = 0$ and deviates from the equilibrium during the decay process. The exciton population of the higher-energy states will decrease due to radiative recombination and transfer to lower-energy sites. However, the decay of excitons is primarily due to transfer processes near the localization threshold and due to radiative recombination processes at the low-energy tail of the emission band. Above E_m , the lifetime of excitons should approach a constant value determined fully by the nonradiative recombination rate due to rapid transfer in extended states.

The mobility edge E_m for CdS_{0.51}Se_{0.49} has been determined from the dependence of the degree of polarization of the exciton luminescence on the excitation energy.¹³ Comparing our emission spectra to the excitation spectrum of polarization degree obtained for CdS_{0.51}Se_{0.49}, we have $E_m \approx 2.095$ eV for CdS_{0.5}Se_{0.5} mixed crystal. At en-

ergies close to E_m , the exciton decay is dominated by the transfer process and is nearly exponential at earlier delay times. The decay rate increases with an increase of emission energy. Figure 2 shows semilogarithmic plots of the exciton luminescence temporal responses ($t_d \geq 0$) for three representative emission energies. We see that the nonexponential decay arises predominantly at longer delay times. With an approximation of exponential decay for earlier times ($t_d \leq 8$ ns), we found that the exciton lifetime as a function of the exciton recombination energy E near the mobility edge can be described by

$$\tau(E) = \tau_0 + \alpha(E_m - E)^\beta \quad (E \leq E_m), \quad (1)$$

with $\beta = 2.1$, $\alpha = 6.58 \times 10^3$ ns/(eV) ^{β} , and $\tau_0 = 0.68$ ns. This behavior is shown in Fig. 3. We think this is a direct consequence of the fact that, at energies close to the mobility edge, the exciton localization radius diverges according to the power law

$$a(E) \sim (E_m - E)^{-s} \quad (E \leq E_m), \quad (2)$$

which is analogous to the behavior of the carriers in the Mott-Anderson localization model. Here E is the exciton recombination energy and $E_m - E$ the exciton localization energy. The calculated critical index s is about $\frac{2}{3}$.^{14,15} However, the critical index s has never been obtained experimentally before. Once an exciton is created at a site where its energy is close to E_m , it will most likely transfer to an available lowest-energy site within its localization volume. The probability of exciton transfer is proportional to the number of available lower-energy sites within the localization volume of excitons, or, equivalently it is proportional to $a^3(E)$. Therefore, we have the dependence of the nonradiative decay time on the exciton localization energy $E_m - E$ as

$$\tau_n = \tau_{n0} + \alpha(E_m - E)^{3s} \quad (E \leq E_m), \quad (3)$$

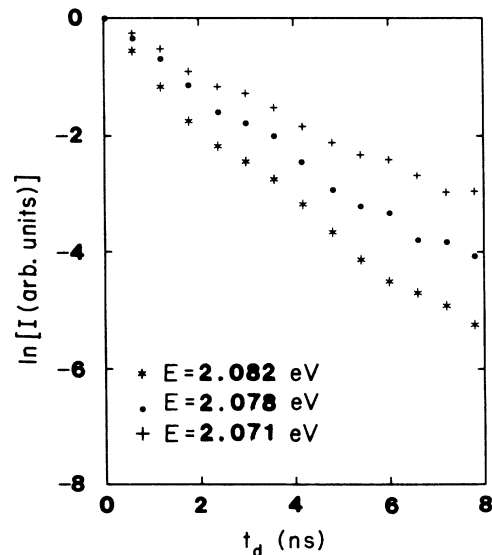


FIG. 2. Semilogarithmic plots of the exciton luminescence temporal responses ($t_d \geq 0$) for three representative emission energies. The data have been normalized to unity at $t_d = 0$.

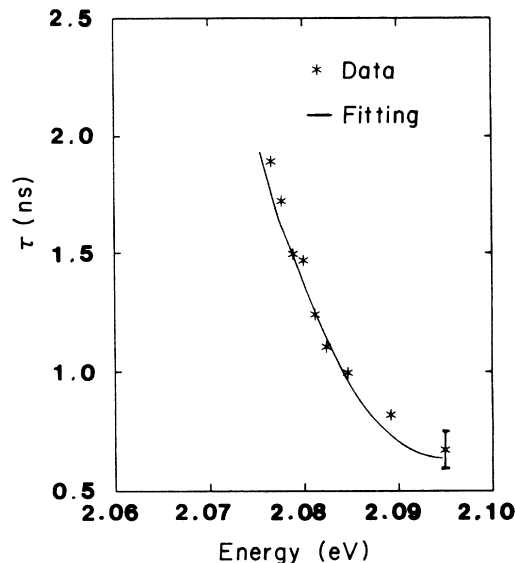


FIG. 3. Experimental values of exciton lifetime determined from exponential decay (asterisks) as a function of emission energy in the vicinity of the spectral peak. The solid line is a least-squares fitting curve using Eq. (1) (see text). Exciton-lifetime deviation (error bar) is shown for one representative emission energy at $E = 2.095$ eV.

where τ_{no} is the nonradiative decay time constant for excitons in the extended states above E_m . The total decay rate is determined by the radiative recombination and the non-radiative recombination. However, the radiative decay time is almost independent of the exciton recombination energy because the potential fluctuations caused by compositional fluctuations are much smaller than the energy gap of the material. The radiative lifetime can be approximated by the exciton lifetime in the low-energy tail of the transition band, which has been measured to be about 3.0 ns,¹⁶ which is much longer than the experimentally measured total exciton lifetime near E_m . Therefore, the observed behavior of the total exciton lifetime is primarily caused by the nonradiative decay due to transfer in this energy region and we can write

$$\tau(E) \approx \tau_{no} + \alpha(E_m - E)^{3s} \quad (E \leq E_m). \quad (4)$$

From Eqs. (1) and (4), experimentally measured β equals $3s$. Therefore, our experimental result of s (equal to 0.7) is in good agreement with the theoretical prediction of $\frac{2}{3}$. This is an experimental demonstration of the Mott-Anderson localization of excitons through the exciton lifetimes. Additionally, we have found an experimental method of measuring the critical index s , which is important for the studies of the critical phenomena in percolative solids.

In the following, we show that the exciton luminescence spectral shift with delay time is correlated to the observed exciton lifetime behavior. In Fig. 4, we plot measured spectral peak positions at different delay times (illustrated by solid circles), which is determined by assuming the luminescence intensity in the vicinity of the peak position (within a few meV) follows a Gaussian distribution. From Fig. 4, we can see that the peak position is at

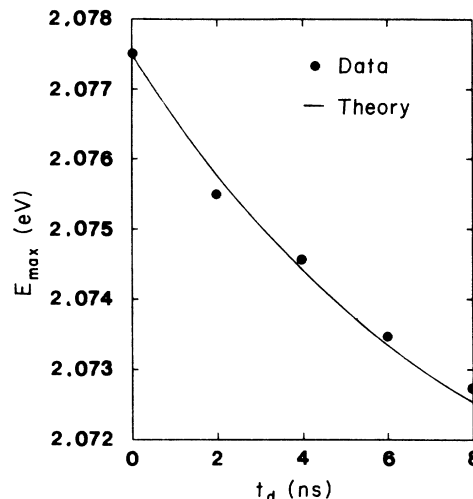


FIG. 4. The spectral peak position (solid circles) as a function of delay time. The solid line is a theoretical calculation result using Eq. (7).

$E = 2.0775$ eV at $t_d = 0$ and shifts to $E = 2.0727$ eV at $t_d = 8$ ns. The exciton luminescence as a function of delay time t_d , and emission energy E , can be assumed to be

$$I(E, t_d) = I_0 \exp \left[-\frac{(E - E_0)^2}{2\sigma^2} - \frac{t_d}{\tau(E)} \right]. \quad (5)$$

Here I_0 and E_0 are, respectively, the maximum intensity of the exciton luminescence and the spectral peak position at $t_d = 0$. σ is related to the FWHM by $\Delta_{FWHM} = 2[2(\ln 2)]^{0.5}\sigma$ and is correlated to the degree of the compositional fluctuations in the crystal. The peak positions at different delay times can be obtained by setting

$$\frac{dI(E, t_d)}{dE} = 0, \quad (6)$$

which gives

$$E_{\max}(t_d) = E_0 + \frac{\sigma^2}{\tau^2(E_{\max})} \left(\frac{d\tau}{dE} \right)_{E_{\max}} t_d. \quad (7)$$

Here we have assumed that the linewidth of the exciton transition is independent of delay time, which is consistent with experimental results shown in Fig. 1. $(d\tau/dE)_{E_{\max}}$ can be obtained from Eq. (1). Equation (7) is plotted in Fig. 4 as a solid line. We see that the calculated results are in good agreement with experimental data. This demonstrates that the exciton spectral shift with delay time is a direct consequence of the exciton-lifetime behavior.

In conclusion, we studied dynamic processes of exciton localization in a $\text{CdSe}_{0.5}\text{S}_{0.5}$ mixed crystal. A power-law dependence of exciton lifetime on localization energy near the mobility edge has been observed, which has been interpreted in terms of the exciton localization radius following the description of the Mott-Anderson localization model. The exciton spectral shift with delay time has been shown to be a more natural consequence of the observed exciton-lifetime behavior.

- ¹D. J. Wolford, B. G. Streetman, S. Lai, and M. V. Klein, *Solid State Commun.* **32**, 51 (1979).
- ²H. Mariette and J. Chevallier, *Solid State Commun.* **29**, 263 (1979).
- ³L. Samuelson, S. Nilsson, Z. G. Wang, and H. G. Grimmeiss, *Phys. Rev. Lett.* **53**, 1501 (1984).
- ⁴E. Cohen and M. D. Sturge, *Phys. Rev. B* **25**, 3828 (1982).
- ⁵S. Sheval, R. Fischer, E. O. Gobel, G. Noll, and P. Thomas, *J. Lumin.* **37**, 45 (1987).
- ⁶J. A. Kash, A. Ron, and E. Cohen, *Phys. Rev. B* **28**, 6147 (1983).
- ⁷M. Oueslati, C. Benoitàla Guillaume, and M. Zouaghi, *Phys. Rev. B* **37**, 3038 (1988).
- ⁸C. Gourdon and P. Lavalland, *Phys. Status, Solidi (b)* **153**, 641 (1989).
- ⁹H. X. Jiang and J. Y. Lin, *Phys. Rev. Lett.* **64**, 2547 (1990).
- ¹⁰H. X. Jiang and J. Y. Lin, *Phys. Rev. B* **40**, 10025 (1989).
- ¹¹J. Y. Lin and H. X. Jiang, *Phys. Rev. B* **41**, 5178 (1990).
- ¹²B. I. Shklovskii and A. L. Efros, in *Electronic Properties of Doped Semiconductors*, Springer Series in Solid-State Sciences Vol. 11, edited by M. Cardona, P. Fulde, and H. J. Queisser (Springer-Verlag, New York, 1984), Chap. 2, and references therein.
- ¹³S. Permogorov, A. Reznitskii, S. Verbin, and V. Lysenko, *Solid State Commun.* **47**, 5 (1983).
- ¹⁴K. F. Freed, *J. Phys. C* **4**, L331 (1971).
- ¹⁵P. W. Anderson, *Proc. Nat. Acad. Sci. USA* **69**, 1097 (1972).
- ¹⁶Experimentally measured exciton lifetimes in the low-energy side saturated and approached $\tau \approx 3.0$ ns at $E = 2.062$ eV.